MEANDERING EARTHQUAKE MOTION OF SOFT SURFACE GROUND

Yutaka Nakamura (I)
Akio Saito (II)
Presenting Author: Y. Nakamura

SUMMARY

This paper deals with the data of meandering earthquake motion observed and with a mathematical model formulated thereupon for analysis of meandering earthquake motion. The mathematical model proposed in this paper was made, based on the concept that attributes the occurrence of the meandering earthquake motion to the difference in dynamic characteristics of each point in the soft layers. It is modeled on the cross-section of layers including the railway track so that the degree of track bending can be calculated.

INTRODUCTION

Usually, the motion of the ground surface in an earthquake is not uniform and varies depending upon the place. Since a straight line drawn on the surface, for example, will move like a snake, this earthquake motion will be refered to as MEANDERING EARTHQUAKE MOTION hereafter.

If the meandering earthquake motion is large, a linear structure like a railway will be bent, which accordingly will cause a problem not only in the structure itself, but also in the safe operation of trains. It is considered that the apparent wavelength and the predominant frequency of the meandering earthquake motion, being problems for railway, are 20 to 80 m and 0.5 to 2 Hz respectively, from the length and the natural frequency of the railway cars and the railway structures.

OUTLINE OF OBSERVATION

The observation stations are located along Anenuma elevated bridge on the Tohoku Line, near Misawa. The ground around is an alluvial flood plain surrounded by diluvial terraces on the three sides except Anenuma side. Anenuma elevated bridge was once damaged by the earthquake motion and ground rupture induced by the 1968 Tokachi-oki Earthquake.

Fig. 1 shows distribution of displacement meters. As illustrated in this figure, eight stations (No. 1 through No. 8) are installed at intervals of 50 to 150 m on the principal traverse line running parallel to the Tohoku Line. The observation components are mainly horizontal component (HT) normal to the principal traverse line, but parallel component (HL) and vertical component (V) are observed loccally, also.

Fig. 2 shows a velocity section along the principal traverse line.

SEISMOGRAMS AND DISCUSSIONS

In order to investigate the relationship between the characteristics of

---

(I) Senior Researcher, Railway Technical Research Institute, Japanese National Railways, Tokyo, JAPAN

(II) Technical Assistant, R.T.R.I., JNR, Tokyo, JAPAN

the meandering earthquake motions and the locations of the epicenters, nine events are selected. Fig. 3 shows distribution of these epicenters.

Wave Propagation and Predominant Frequency

Fig. 4 are the seismograms of No. 29 and No. 38 earthquakes. All these waveforms are horizontal displacement of HT component. By the similarity of waveforms, the stations are classified into three categories: No. 1 through No. 3 stations where the thickness of soft surface ground is approximately 20 m; No. 6, No. 7 and No. 9 stations where the thickness of soft surface ground is approximately 7 m; and No. 4 and No. 5 stations where the thickness of soft surface ground lies between the former two categories.

The epicenter of No. 29 earthquake was located in the direction of the principal traverse line. Assuming that the propagation velocity of the seismic wave had been on a level with that through the soft surface layers, the seismic wave should have taken approximately 10 sec to travel the 450 m span between No. 2 and No. 7 stations. According to Fig. 4 (a), however, the propagation time difference is less than 1 sec on the average, showing that the seismic waves may have propagated through the stations at a velocity of more than 500 m/s.

As regards No. 38 earthquake, using the cross-correlation functions, the propagation time differences were determined. From the propagation time differences between No. 2, No. 6 and No. 9 stations forming a triangle, the inputting direction and the velocity of seismic wave propagation were calculated. The inputting direction is nearly the epicenter azimuth with an error of approximately 10°, and the propagation velocity is estimated at 900 m/s. Fig. 5 is a travel time curve obtained on assumption that the seismic wave inputting direction is in line with the epicenter. From the predominant period of the cross-correlation functions, it is inferred that the travel time curve in Fig. 5 may represent the waves with a period of approximately 4 sec.

Fig. 6 shows Fourier spectra of the observed displacements at No. 2 through No.7 stations when No. 29 earthquake occurred. According to Fig. 6, the earthquake ground motions up to 1 Hz are predominant at these stations. The 0.25 Hz wave peaks at almost every station, and the waves of 0.5 Hz and 0.75 Hz peak at No. 2 through No. 4 or No. 5 stations. Considering the result of a microtremor measurement at No. 1 through No. 4 stations that 0.5 Hz and 0.75 Hz waves always prevail, these waves may be considered to have due to the soft surface layer. On the other hand the 0.25 Hz wave is common to all the seismic stations, and its propagation velocity is far and away faster than the corresponding velocity through the soft layer; namely, it is considered to have a close relation with the deeper geological structure.

Meandering Earthquake Motion

Fig. 7 shows examples of the deformation mode of the principal traverse line (instantaneous mode) due to eight earthquakes. According to Fig. 7, it is found that the zero points where the amplitudes are almost zero form a line. Taking this line as representative of an apparent wave propagation, it happens that the propagation is from No. 2 station toward No. 7 station if the line falls rightwards, and that the propagation is from No. 7 station to No. 2 station if the line falls as it goes leftwards. As regards 0.5 Hz, 0.75 Hz and 1.5 Hz, the pattern is not so clear as to show that the propagation of zero points unidirectional. As for 1 Hz and 1.25 Hz, however, the zero point propagation is evident, and its velocity is in excess of 500 m/s, far faster

than the surface shear wave propagation velocity. It is to be noted, however, that even in case of zero point propagation, the propagation of large amplitude is quite limited. The phenomenon above is observed whether the epicenters are located normal to the principal traverse line or not. Taken altogether, it may be concluded that the meandering earthquake motions of the soft surface layer are caused by the multiple vertical reflections of those waves within the soft surface layer which are propagated horizontally in the deeper and harder base ground and then inputted into the bottom of the soft surface layer, rather than the waves propagating horizontally along the soft surface layer.

As regards the degrees of the earthquake ground motion, the horizontal components are far larger in amplitude than the vertical components as illustrated in Fig. 8.

MATHEMATICAL MODEL FOR MEANDERING EARTHQUAKE MOTION

We judged from the characteristics of meandering earthquake motions discussed above that the meandering motions are due primarily to the phase difference resulting from difference in dynamic characteristics of each point on the surface layer, and formulated a mathematical model as discussed hereunder. What interests us most is the ground displacement behavior across the railway because our primary objective is to collect basic data upon which to evaluate the aseismicity and the trafficability of the railway structures. For this reason, we prepared a mathematical model to estimate the earthquake ground motion along the railway. This model is composed finite elements which are free to move only in the directions normal to the railway. Fig. 9 shows a prismatic finite element. The element is movable along the rigid ridge line of the trigonal prism. The element stiffness matrix [K] is formed by taking into account the shear deformation alone of this element.

The displacement w within the element is expressed by the following formula:

$$w = a_1 + a_2 x + a_3 y \tag{1}$$

where indefinite constants, a_1, a_2 and a_3, are determined by the displacement of three edges.

$$\begin{pmatrix} a_1 \\ a_2 \\ a_3 \end{pmatrix} = \begin{pmatrix} 1 & x_1 & y_1 \\ 1 & x_2 & y_2 \\ 1 & x_3 & y_3 \end{pmatrix}^{-1} \begin{pmatrix} w_1 \\ w_2 \\ w_3 \end{pmatrix} \tag{2}$$

By substituting equation (2) into equation (1), we obtain the displacement w as follows:

$$w = [L_1 \; L_2 \; L_3][w_1 \; w_2 \; w_3]^T \tag{3}$$

where, $L_i(x, y) = [(xy_j + x_j y_k + x_k y) - (yx_j + y_j x_k + y_k x)]/A$

$(i,j,k) = (1,2,3), (2,3,1), (3,1,2);$

A is the area of the elemental triangle.

As the shear displacement in the z-direction alone considered, the stress is given by the following formula:

$$\begin{pmatrix} \varepsilon_z \\ \gamma_{xz} \\ \gamma_{yz} \end{pmatrix} = \begin{pmatrix} \partial w/\partial z \\ \partial w/\partial x + \partial u/\partial z \\ \partial w/\partial y + \partial v/\partial z \end{pmatrix} = \begin{pmatrix} 0 \\ \partial w/\partial x \\ \partial w/\partial y \end{pmatrix} \tag{4}$$

By substituting equation (3) into equation (4), we obtain the following:

$$\{\varepsilon\} = \begin{Bmatrix} \gamma_{xz} \\ \gamma_{yz} \end{Bmatrix} = (1/A) \begin{bmatrix} y_2-y_3 & y_3-y_1 & y_1-y_2 \\ x_3-x_2 & x_1-x_3 & x_2-x_1 \end{bmatrix} \begin{Bmatrix} w_1 \\ w_2 \\ w_3 \end{Bmatrix} = [B]\{u\} \tag{5}$$

The stress strain relationship is given by the following formula:

$$\{\sigma\} = \begin{Bmatrix} \tau_{xz} \\ \tau_{yz} \end{Bmatrix} = \begin{bmatrix} G & 0 \\ 0 & G \end{bmatrix} \begin{Bmatrix} \gamma_{xz} \\ \gamma_{yz} \end{Bmatrix} = [D]\{\varepsilon\} \tag{6}$$

Thus, the equation of equilibrium of element is given as follows:

$$\{F\} = [K]\{u\}$$

where, $\{F\} = \{f_1 \ f_2 \ f_3\}^T$

$$[K] = \int [B]^T[D][B]dV = [B]^T[D][B]At \tag{7}$$

t : thickness of element.

The mass matrix used is a lumped mass matrix in which the mass of an element is divided into three equall parts for allocation to respective edges.

By the way convinience, this method is termed the SHEAR-FEM. The motion of a railway in the crosswise direction can be studied by application of the SHEAR-FEM to profile model of the railway. As each node has one degree of freedom, or half the number of degrees of freedom usually assigned to two-dimensional FEM, the memory load on the computer can be reduced to a quarter.

Fig. 10 is a profile model of Anenuma observation stations along the Tohoku Line. It is refers to the layers within which Vs is less than 250 m/s. On the ground surface, the nodal pitch is 5 m. The total number of degrees of freedom is 294. The seismic response is calculated according to the modal analysis.

ESTIMATION OF GROUND MOTIONS IN ANENUMA DUE TO THE 1968 TOKACHI-OKI EARTHQUAKE

Here we shall estimate the ground motion at Anenuma elevated bridge due to the 1968 Tokachi-oki Earthquake (M = 7.9, h = 0 km), and shall compare it with the actual deformation of Anenuma elevated bridge. Fig. 11 shows the deformation of Anenuma elevated bridge due to the 1968 Tokachi-oki Earthquake. The linear response analysis is incapable of explaining out the residual deformation of the elevated bridge directly, but it is no doubt that those parts which leave markes of heavy distortion must have been subjected to vibrations with a large amplitude. For the sake of indirect analysis, we shall use the obseved surface accelerogram of EW-component at Hachinohe near Anenuma, as converted accelerogram in the basement (17 m deep) where Vs is approximately 400 m/s, or almost the same as that in the basement of Anenuma. Fig. 12 shows a converted basement accelerogram. As it is inferred that the extremely soft layer (Vs = 14 m/s) and its neighborhood will experience a considerably large strain, the calculation is made with their rigidity reduced to 1/2 and 1/4 of the initial value.

Fig. 13 is the instantaneous modes of response waveforms, showing that with the reduction in rigidity, the response displacement lowers and at the same time the apparent wavelength gets shorter. The actual residual deformation at No. 3 and No. 5 stations are 75 cm and 68 cm, respectively. The calculation also shows peaks at No. 3 and No. 5 stations, and the envelope

of the displacement waveform bears a close resemblance to the actual residual deformation. The calculation shows a maximum response of 84 cm for the initial rigidity, but the response lowers with decreese in rigidity, though it remains comparable with the actual residual deformation. As it is logical to consider that the larger the vibration amplitude is, the larger the residual deformation will be.

It is also noteworthy here that the meandering earthquake motions are pronounced where the thickness of soft surface layer is changed sharply or where the extremely soft layer exists.

CONCLUSION

We have discussed the observed meandering earthquake motions and the mathematical model (SHEAR-FEM) developed based upon them. We have applied this model for estimation of surface ground motion at Anenuma due to the 1968 Tokachi-oki Earthquake, with the following results:

(1) SHEAR-FEM is effective in estimation of the meandering earthquake motion,
(2) The meandering earthquake motion became violent where the thickness of soft layer changes or where the extremely soft layer localizes.

ACKNOWLEDGEMENTS

This study was carried out as a part of studying commitee for earthquake-resistant reainforcement of railway structures of JNR (the chairman is Dr. Shunzo Okamoto). Our gratitude are expressed to the chairman and other member for their valuable advices and fruitful discussions.

BIBLIOGRAPHY

(1) Nakamura, Y. and Saito, A.: HIGH-DENSITY ARRAY OBSERVATION OF EARTHQUAKE MOTION IN SOFT GROUND (in japanese), Proc. of the 16th JCEE,1981,pp.41-44.
(2) Nakamura, Y. and Saito, A.: MEANDERING EARTHQUAKE MOTION OF SOFT GROUND (in japanese), Proc. of the 6th JEES, 1982, pp.441-448.
(3) Tsuchida, H.,Kurata, E. and Sudo, K.: STRONG MOTION EARTHQUAKE RECORDS ON THE 1968 TOKACHI-OKI EARTHQUAKE AND ITS AFTERSHOCKS, Technical Notes of the Port and Harbour Research Institute, No. 80, 1969, pp.205-266.

FIGURES

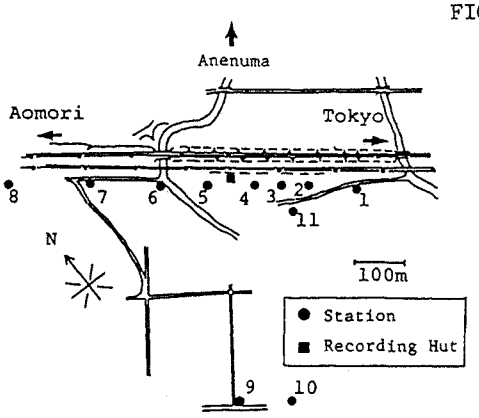

Fig.1 Array of Stations at Anenuma

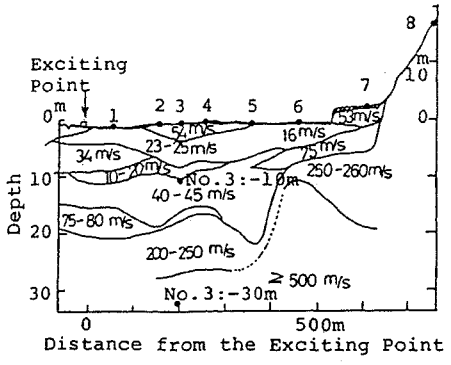

Fig.2 Profile of Strata along the Principal Traverse Line

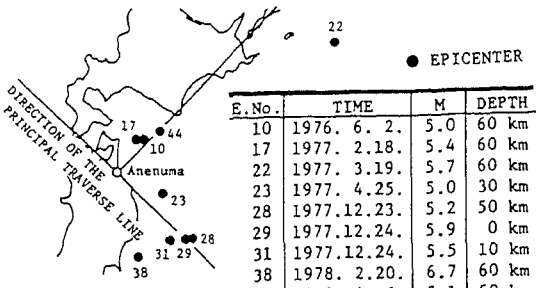

E.No.	TIME	M	DEPTH
10	1976. 6. 2.	5.0	60 km
17	1977. 2.18.	5.4	60 km
22	1977. 3.19.	5.7	60 km
23	1977. 4.25.	5.0	30 km
28	1977.12.23.	5.2	50 km
29	1977.12.24.	5.9	0 km
31	1977.12.24.	5.5	10 km
38	1978. 2.20.	6.7	60 km
44	1978. 4. 6.	5.1	50 km

Fig.3 Distribution of Epicenters

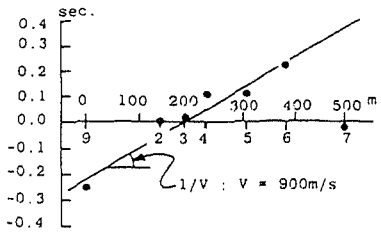

Fig.5 Travel-Time Curve of No.38 Earthquake

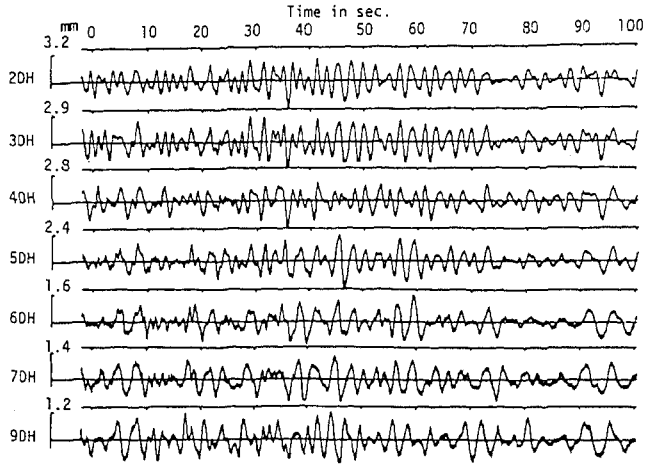

(a) No.29 Earthquake

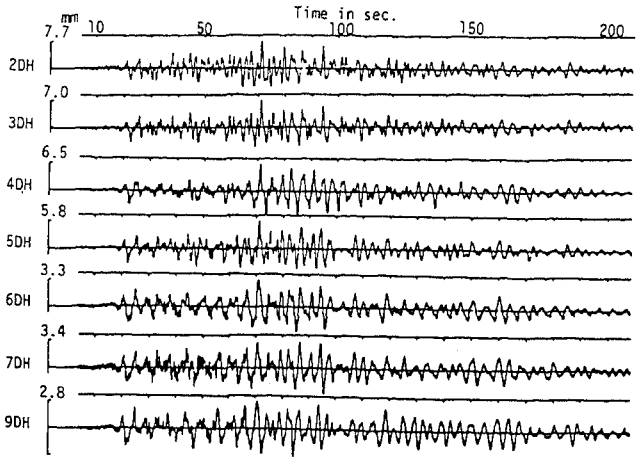

(b) No.38 Earthquake

Fig.4 Seismograms of No.29 & No.38 Earthquakes

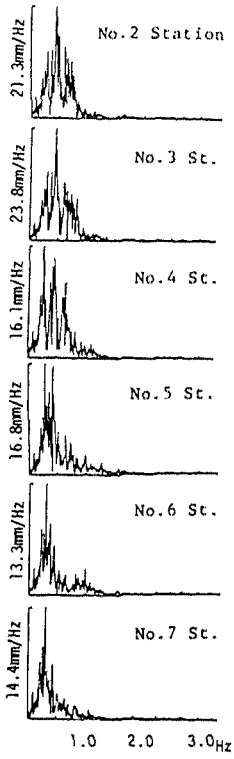

Fig.6 Fourier Spectra of No.29 Earthquake

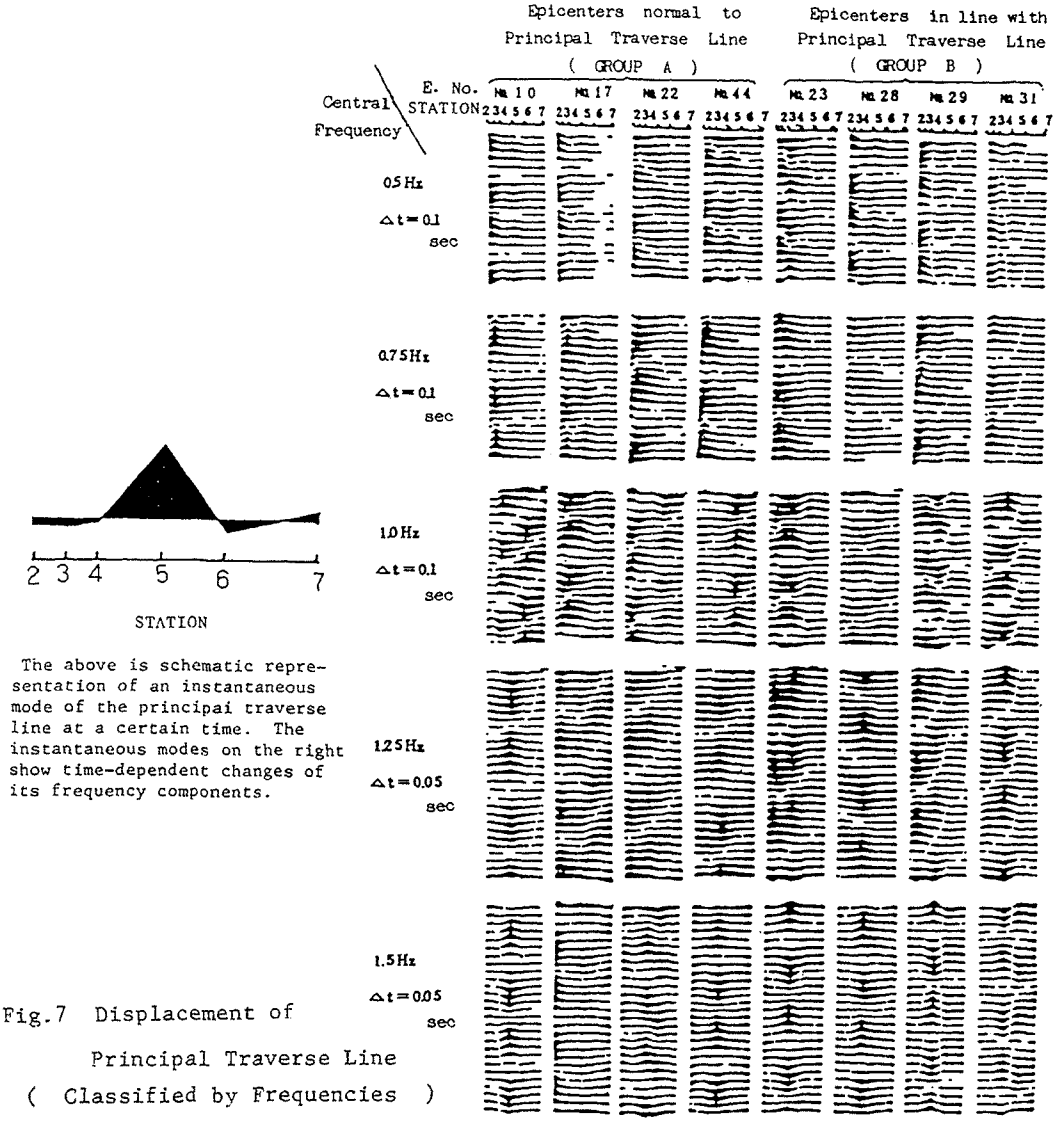

The above is schematic representation of an instantaneous mode of the principai traverse line at a certain time. The instantaneous modes on the right show time-dependent changes of its frequency components.

Fig.7 Displacement of Principal Traverse Line (Classified by Frequencies)

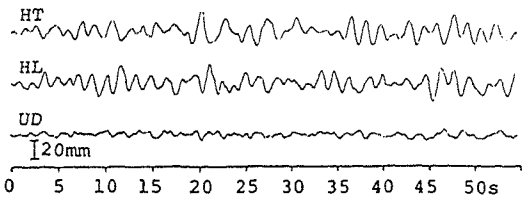

Fig.8 Three Components of Surface Ground Motion by Urakawa Earthquake (1982. 3.21, M=7.1, h=40km, =180km)

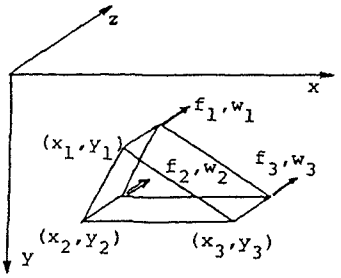

Fig.9 Two Dimensional Element

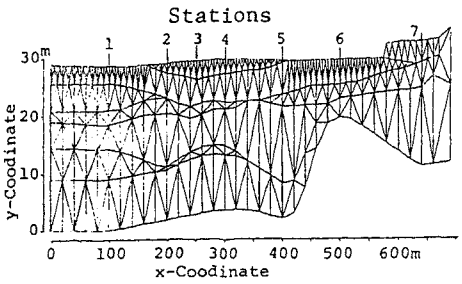

Fig.10 FEM Mesh of Ground

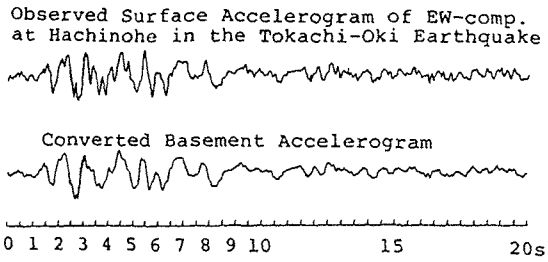

Fig.12 Basement Accelerogram

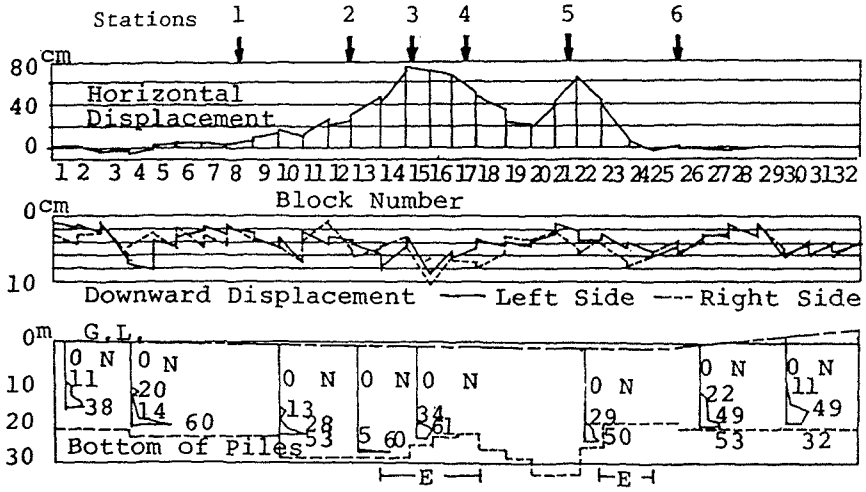

E: The Location where Embankment Sunk
N: Number of Blows per 30cm in Standard Penetration Test

Fig.11 Damage of Anenuma Elevated Bridge by the 1968 Tokachi-oki Earthquake

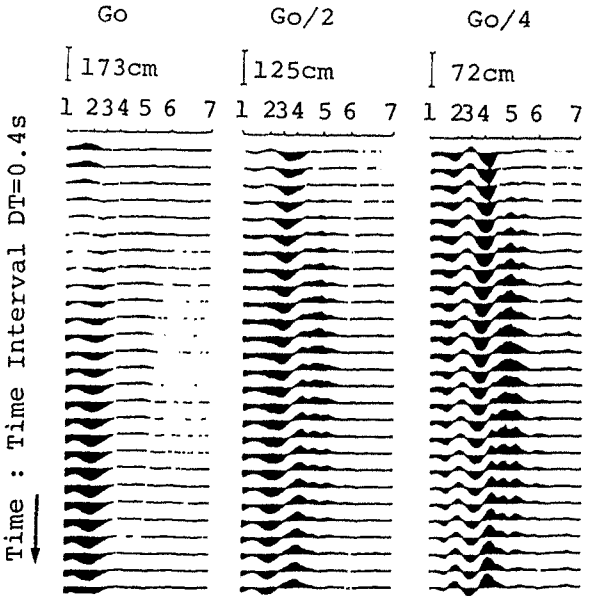

Fig.13 Estimated Instantaneous Modes
(Input: Hachinohe EW-comp.)